# Understanding the Spatiotemporal Structures in Atmosphere-Land Surface Exchange at the Jülich Observatory for Cloud Evolution (JOYCE)

**Marke**[1], T., S. Crewell[1], U. Löhnert, J. Schween, and U. Rascher[2]

*[1] Institute of Geophysics and Meteorology, University of Cologne, [2] Institute of Bio- and Geoscience, Research Center Jülich*

## 1. Introduction to the Measurement Site

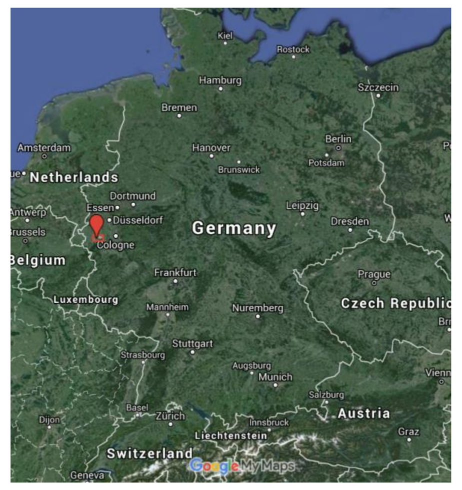

*Fig. 1: Location of the JOYCE site in Jülich, Germany.*


***Fig. 2:*** *Examples of JOYCE instruments (left to right): Doppler Lidar, Microwave Radiometer, Ceilometer, Cloud Radar,120 m Meteorological Tower and Eddy Covariance station*

Continuous and temporally highly-resolved measurements of the **cloudy boundary layer** are provided at the Jülich Observatory for Cloud Evolution (**JOYCE**, Fig. 1) since 2011, by using ground based passive and active remote sensing and in-situ instruments (Fig. 2).

## 2. Site Characterization with Ground Based Observations

- Macro-physical properties of boundary layer clouds are assessed with the **synergy** of a ceilometer and cloud radar.
- ➢ High monthly variability of the **total cloud cover** (Fig. 3)

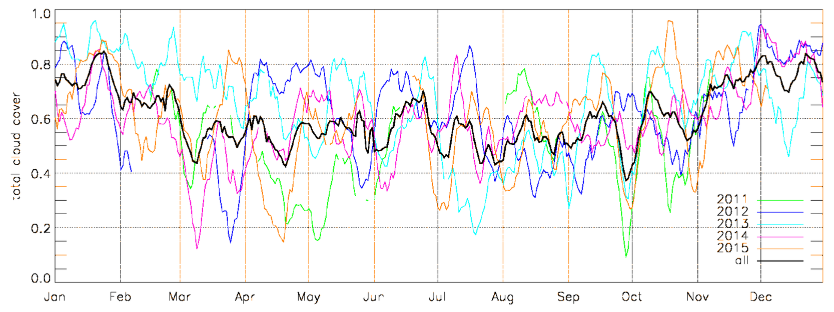

***Fig. 3:*** *Daily mean total cloud cover at JOYCE using a Ceilometer (10 day center moving average)*

- Comparison of remote sensing, in-situ and model derived **wind direction** (Fig. 4)
- ➢ Influences of the local and synoptic scale can be identified

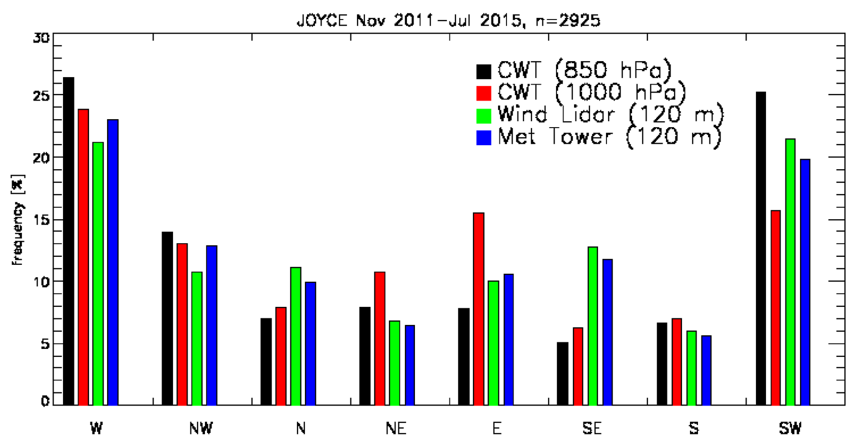


***Fig. 4:*** *Wind direction derived from Doppler Lidar and Meteorological Tower (120 m) and Circulation Weather Type Classification based on ERA-Interim 850 hPa / 1000 hPa.*

- **Azimuth scans** using a microwave radiometer (Fig. 5) provide the spatial distribution and gradient of the **integrated water vapor (IWV)**.
- ➢ Link to exchange processes of the surface (Fig. 11)

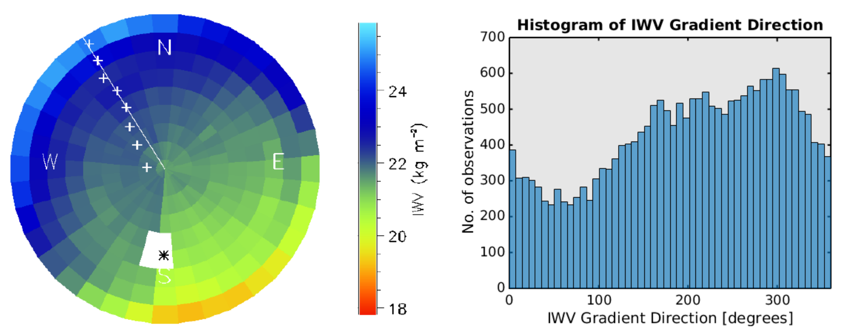


***Fig. 5:*** *Left: Air mass corrected IWV field and IWV gradient derived from one microwave radiometer hemispheric scan. Right: IWV gradient direction histogram.*

## 3. A Scheme to Classify the Cloudy Boundary Layer

By reducing the observations of the boundary layer (BL) into a specific set of types helps understanding the **evolution of mixing processes** in the lowest part of the troposphere. Furthermore, the turbulence can be identified as cloud or surface driven (Harvey et al., 2013).

**Doppler Lidar**
- Vertical stare
- 3 beam swinging method

**Eddy Covariance station**
- Sonic anemometer vertical wind
- Sonic temperature

**Preprocessing and Derivation of Parameters**
- Background shape and ripple correction
- Calculate parameters:
  - Cloud/aerosol layers
  - Vertical wind Skewness
  - Dissipation rate
  - Vector wind shear
  - Sensible heat flux
- Combine all parameters at common resolution

**Boundary Layer Classification**

***Fig. 6:*** *Schematic representation of the boundary layer classification.*

### Preprocessing of Doppler Lidar Data

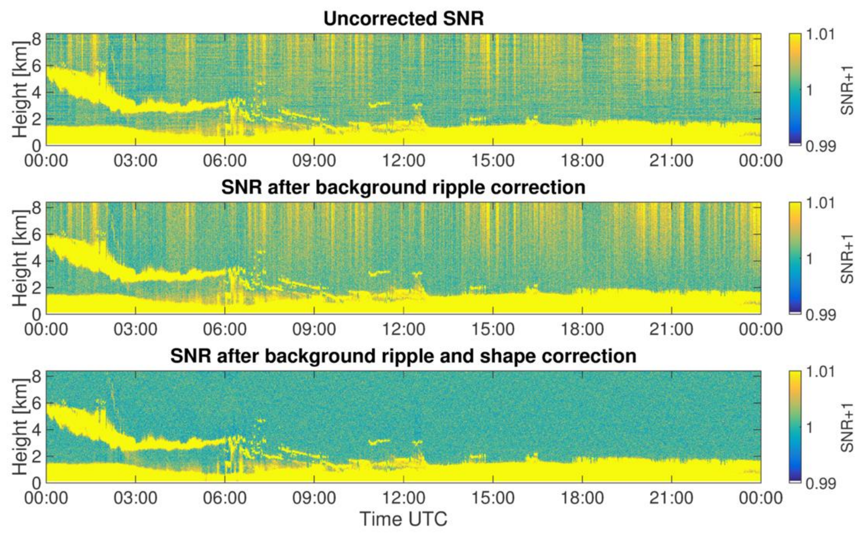


***Fig. 7:*** *Doppler Lidar SNR before and after correction.*

Background shape correction (Manninen et al., 2015) and ripple correction (Vakkari et al., to submit)

- ➢ Homogeneous background
- ➢ Allows lower signal-to-noise ratio (SNR) threshold
- ➢ Bias in turbulent properties is reduced

### Observations Used for the Classification

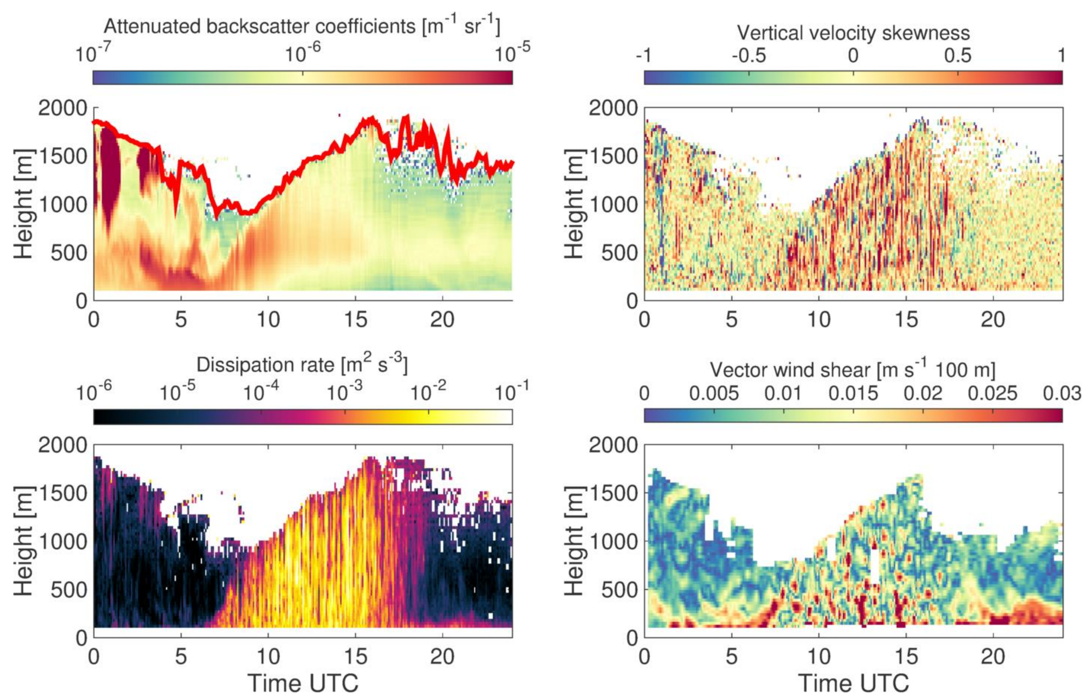


***Fig. 8:*** *Time series of the attanuated backscatter coefficient, vertical velocity skewness, dissipation rate and vector wind shear (clockwise from top left).*

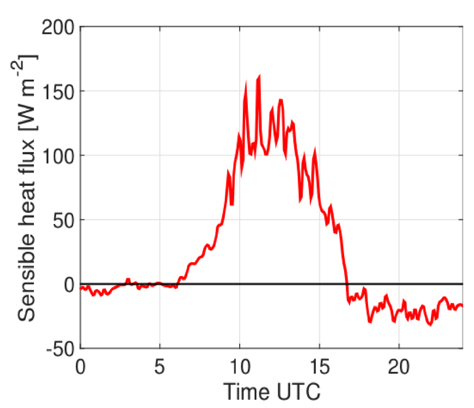


***Fig. 9:*** *Time series of the sensible heat flux derived from the EC station.*

## 4. Boundary Layer Classification Results

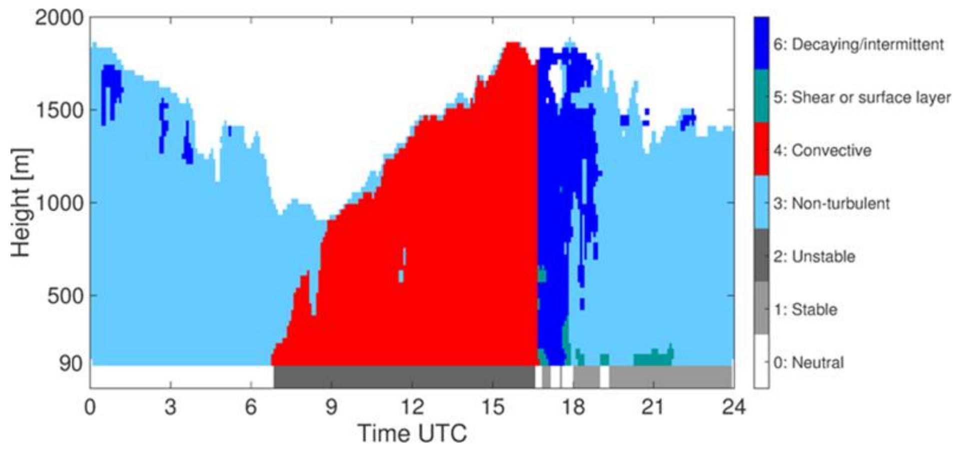


***Fig. 10:*** *Illustration of the bit-field, showing the boundary layer classification.*

- Each pixel in the common resolution grid (temporal: 5 min, vertical: 30 m) is classified using a **bit-field**.
- Type decisions are based on combinations of **threshold** values (Table 1)

| Parameter | Attenuated backscatter coefficient | Vertical velocity skewness | Dissipation rate | Vector wind shear | Sensible heat flux |
|---|---|---|---|---|---|
| **Threshold** | $10^{-5}$ | 0 | $10^{-4}$ m$^2$ s$^{-3}$<br>$10^{-3}$ m$^2$ s$^{-3}$ | 0.02 m s$^{-1}$<br>per 100 m | 0 W m$^{-2}$<br>±10 W m$^{-2}$ |

***Table 1:*** *Thresholds used for the bit-field.*

**Outlook**: Operational use in the **Cloudnet** (Illingworth et al., 2007) framework.

## 5. Further Applications of the BL Classification

- **HyPlant**: high-resolution airborne imaging spectrometer for vegetation monitoring (sun-induced and chlorophyll **fluorescence**, Fig. 11)
- ➢ Link between IWV scans and surface patterns

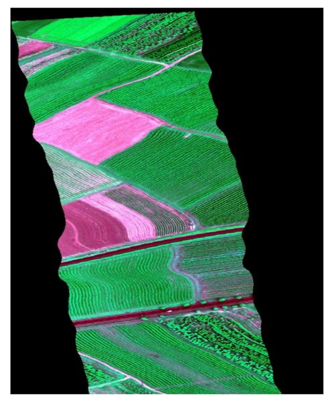

***Fig. 11:*** *HyPlant fluorescence imager (670-780 nm) with a 3 m resolution*

- **ICON** (ICOsahedral Nonhydrostatic): unified modeling system for global numerical weather prediction (NWP) and climate studies that performs as a large eddy simulation (**LES**) model (Fig. 12)
- ➢ Evaluate BL type parameterizations

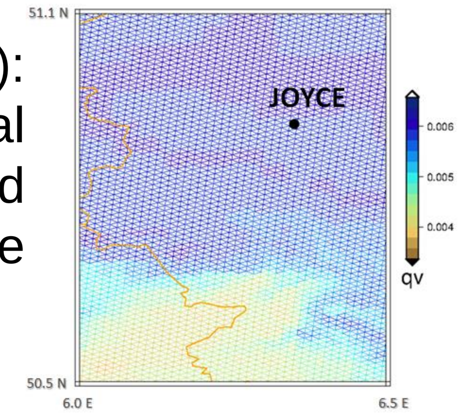


***Fig. 12:*** *Water vapor mixing ratio qv (kg/kg) from a ICON model run at around 800 m height with a 624 m horizontal resolution*

**References:**

Dipankar, A., B. Stevens, R. Heinze, C. Moseley, G. Zängl, M. Giorgetta, and S. Brdar, 2015: Large eddy simulation using the general circulation model ICON, J. Adv. Model. Earth Syst., 7, 963-986.

Harvey, N. J., R. J. Hogan, and H. F. Dacre, 2013: A method to diagnose boundary-layer type using Doppler lidar, Q. J.R. Meteorol. Soc., 139, 1681-1693.

Illingworth, A. J., and Coauthors, 2007: Cloudnet: Continuous evaluation of cloud profiles in seven operational models using ground-based observations. Bull. Amer. Meteor. Soc., 88, 883-898.

Manninen, A. J., E. J. O'Connor, V. Vakkari, and T. Petäjä, 2015: A generalised background correction algorithm for a Halo Doppler lidar and its application to data from Finland, Atmos. Meas. Tech. Discuss., 8, 11139-11170.



tmarke@meteo.uni-koeln.de